Ref [10]

PHYSICAL REVIEW A VOLUME 41, NUMBER 4 15 FEBRUARY 1990

Finite-size effects on the characterization of fractal sets: $f(\alpha)$ construction via box counting on a finite two-scaled Cantor set

Jan Håkansson
Nordisk Institut for Teoretisk Atomfysik, Blegdamsvej 17, DK-2100 Copenhagen Ø, Denmark and Institute of Theoretical Physics, Chalmers University of Technology, S-412 96 Göteborg, Sweden

Gunnar Russberg
Nordisk Institut for Teoretisk Atomfysik, Blegdamsvej 17, DK-2100 Copenhagen Ø, Denmark
(Received 11 September 1989)

We study box counting on finite fractal sets and investigate how to obtain the generalized dimensions and the spectrum of scaling indices with highest possible accuracy. As a model we use a simple one-dimensional Cantor set for which the $f(\alpha)$ spectrum may be found analytically—the exact result is compared with the box-counting solution on the finite levels. There is a connection between the q value and the size of the boxes giving the most accurate result for the $f(\alpha)$ spectrum on any finite level.

I. INTRODUCTION

During the last few years it has become clear that most fractals in nature are so-called multifractals. This means that the characteristic scaling properties of an object may vary from point to point. For this reason the *Hausdorff dimension,* which has extensively been used as a quantitative measure of the scaling in simple fractal objects, is not sufficient to characterize a multifractal. The Hausdorff dimension is only one in a continuum of dimensions, the *Renyi dimensions* D_q,[1] introduced by Grassberger[2] and Hentschel and Procaccia[3] in order to characterize fractals and strange attractors. In this formalism, D_0 is identical to the Hausdorff dimension, while D_1 and D_2 are known as the *information dimension* and the *correlation dimension,* respectively. A similar characterization is obtained by the spectrum of scaling indices, the $f(\alpha)$ spectrum, defined by Halsey *et al.*[4] The generalized dimensions D_q and the $f(\alpha)$ spectrum are related to each other via a Legendre transformation.

Real fractal objects, like aggregates, show fractal properties only within a limited length scale interval. Such *finite* fractals may consist of a finite number of objects with finite sizes. The structure becomes nonfractal inside the single particles as well as outside some typical correlation length. The *practical* determination of the scaling properties of an experimentally obtained fractal object will generally involve box counting on a two-dimensional image (e.g., a projection, like a transmission electron micrograph of aggregated Co particles[5]). When partitioning such an image, the effect of finite particle size will play an important role for the determination of the $f(\alpha)$ spectrum, especially for negative values of q (see below); the calculation of $f(\alpha)$ for negative q has proven to be a difficult problem and a straightforward box-counting calculation will yield completely irrelevant spectra.[6–8] This is due to the finite resolution and to the fact that the boxes will not be necessarily centered on particles of the fractal; some of them will contain vanishingly small measure giving unreasonably large contributions as q is taken to minus infinity (the measure is being raised to the power of q, see below).

In general, it is not possible to identify single particles in an observed image. Instead one may *define* a smallest "particle" size, or *resolution,* being an estimate of the size of the smallest observable single particle, and then create a new image built up of these "particles." This procedure gives a smallest relevant grid size for the box counting; on the particle scale, each box will completely cover one particle and thus have a uniform measure. If the image is digitized there is a natural finest resolution given by the digitization grid.

A number of digitizations with different grid sizes may be constructed from an original image in order to create images with varying degrees of resolution. Alternatively, new digitizations may be obtained from the original one by some appropriate construction rule. This will be discussed for one- and two-dimensional images in a later work. The basic idea is that by computing a set of (optimal) $f(\alpha)$ approximations for different degrees of resolution, an extrapolation beyond the approximation obtained for the finest possible resolution will yield a good estimate of the $f(\alpha)$ spectrum corresponding to infinitely fine resolution.

In this work we will study the effect of finite particle size on box-counting construction of the $f(\alpha)$ spectrum. We use a simple two-scaled Cantor set to model a finite one-dimensional fractal with varying degrees of resolution, and we show how to obtain on each level of resolution the optimal $f(\alpha)$ approximation for both positive and negative q. The approximations are compared with the exact $f(\alpha)$ spectrum for the (infinite) Cantor set (calculated below). The complication of noncentered boxes is automatically eliminated by the choice of set construction; how to best avoid partially covered boxes for a general experimental fractal image will be a subject of the continued work.

II. GENERAL FORMALISM

The starting point in the analysis of fractal objects, such as aggregates, strange attractors, and other complex sets, is the construction of a partition function Γ. Divide the set into N pieces with a size l_i and a probability weight p_i of the ith piece. The partition sum is then given by[4]

$$\Gamma(\tau,q)=\sum_{i=1}^{N}\frac{p_i^q}{l_i^\tau} . \tag{1}$$

As $l\equiv\max(l_i)\to 0$, three things may happen: (i) If $\tau>\tau(q)$, the partition sum diverges; (ii) if $\tau<\tau(q)$, the partition sum becomes zero; only when (iii) $\tau=\tau(q)$, the partition sum may approach a finite, nonzero value. Thus, by requiring $\Gamma(\tau,q)=$const, we define the relation between τ and q. The new dimensions $\tau(q)$ are simply related to the generalized dimensions D_q through[4]

$$\tau(q)=(q-1)D_q . \tag{2}$$

Now, assume the following scaling relation for the probability of the ith piece in the limit $l\to 0$:

$$p_i\sim l^{\alpha_i} . \tag{3}$$

This relation defines the scaling index α_i. The same scaling relation may be found in many points, and all points on the multifractal having the same scaling index are said to be a subfractal with a pointwise dimension α_i. This subfractal has the dimension $f(\alpha_i)$. In other words, the function $f(\alpha)$ can be interpreted as the Hausdorff dimension of the set of points with the same pointwise dimension α. For a simple fractal, e.g., a self-similar object like a one-scaled Cantor set (not multifractal) $f(\alpha)=D_0$ for $\alpha=D_0$, and zero elsewhere, whereas for a multifractal α assumes values over an interval and $f(\alpha)$ is a continuous function on this interval. If we now divide the system into pieces of size l and express the partition sum (1) as an integral over α, we get

$$\Gamma(\tau,q)=l^{-\tau}\int d\alpha'\rho(\alpha')l^{q\alpha'-f(\alpha')} , \tag{4}$$

where $d\alpha'\rho(\alpha')l^{-f(\alpha')}$ is the number of times α' assumes a value in the interval $[\alpha',\alpha'+d\alpha']$. In the limit $l\to 0$, the dominant contribution to the integral is received when the exponent $q\alpha'-f(\alpha')$ is close to its minimum value, so we perform a saddle-point approximation

$$\frac{d}{d\alpha'}[q\alpha'-f(\alpha')]_{\alpha'=\alpha(q)}=0 . \tag{5}$$

This leads to the following Legendre transformation,[4] which is used to determine $f(\alpha)$:

$$\frac{d\tau}{dq}=\alpha , \tag{6}$$

$$\tau(q)=\alpha q-f , \tag{7}$$

$$\frac{df}{d\alpha}=q , \tag{8}$$

$$\frac{d^2f}{d\alpha^2}<0 . \tag{9}$$

From Eqs. (8) and (9) we note that the $f(\alpha)$ spectrum is a convex function with a slope q in each dense point. As $q\to\infty$ the largest p_i (i.e., the most concentrated part of the multifractal) dominates the partition sum. This corresponds to a point where the $f(\alpha)$ curve vanishes with infinite slope, and where α has its minimum value. As $q\to-\infty$ the smallest p_i dominates and at the corresponding maximum α value the $f(\alpha)$ curve vanishes with negative infinite slope. We also note that the maximum value of $f(\alpha)$ is equal to the Hausdorff dimension since $f(\alpha)$ has its maximum for $q=0$ and $D_0=-\tau(0)$.

III. EXACT RESULTS FOR TWO-SCALED RECURSIVE SETS

If a measure is constructed from an exact recursive rule, one can easily determine its $\tau(q)$, D_q, and $f(\alpha)$ spectrum. Suppose that the measure is generated by the following process. Start with the original region with measure one and size one. Divide the region into pieces of two sizes and probabilities, where N of them are nonempty. Let n_1 denote the number of pieces of length l_1 and n_2 the number of length l_2. Further, let the respective probabilities be p_1 and p_2. At this first level the partition sum is given by

$$\Gamma_1=n_1\frac{p_1^q}{l_1^\tau}+n_2\frac{p_2^q}{l_2^\tau} , \tag{10}$$

where $n_1+n_2=N$. To get the next level of the set, each piece is further divided into N nonempty pieces. At this second level the partition sum will be

$$\Gamma_2=n_1^2\left[\frac{p_1^q}{l_1^\tau}\right]^2+2n_1n_2\frac{p_1^q}{l_1^\tau}\frac{p_2^q}{l_2^\tau}+n_2^2\left[\frac{p_2^q}{l_2^\tau}\right]^2=\Gamma_1^2 . \tag{11}$$

We now see that the first partition function will generate all the others and $\Gamma_n=\Gamma_1^n$. For this reason Γ_1 is called a *generator* for the set.[9] If the probabilities are normalized ($n_1p_1+n_2p_2=1$), then $\tau(q)$ is defined through $\Gamma_n(q,\tau)=1$. This gives us the following equation (which can be solved numerically) for determining $\tau(q)$:

$$n_1\frac{p_1^q}{l_1^\tau}+n_2\frac{p_2^q}{l_2^\tau}=1 . \tag{12}$$

If we for simplicity choose the lengths l_1 and l_2 such that $l_1=L$ and $l_2=l=L^2$ and the probabilities to be proportional to the corresponding box size, i.e., $p_1=L^d/(n_1L^d+n_2L^{2d})$ and $p_2=L^{2d}/(n_1L^d+n_2L^{2d})$, where d is the geometrical (Euclidean) dimension of the set, we can rewrite Eq. (12) as a second-order equation in $L^{dq-\tau}$. The solution to this equation gives

$$\tau(q)=dq-\frac{1}{\ln L}\ln\left[\frac{(n_1^2+4n_2\gamma^q)^{1/2}-n_1}{2n_2}\right] , \tag{13}$$

where

$$\gamma=n_1L^d+n_2L^{2d} . \tag{14}$$

From the relation (2) the whole spectrum of generalized dimensions is known as well. In particular, the values of

$D_{-\infty} \equiv \alpha_{\max}$ and $D_{\infty} \equiv \alpha_{\min}$ are given by

$$D_{-\infty} = d - \frac{\ln\gamma}{2\ln L} = \frac{\ln p_2}{2\ln L} \tag{15}$$

and

$$D_{\infty} = d - \frac{\ln\gamma}{\ln L} = \frac{\ln p_1}{\ln L} \ . \tag{16}$$

Equations (6) and (7) give us the $f(\alpha)$ spectrum

$$\alpha(q) = d - \frac{\gamma^q \ln\gamma}{\ln L} \frac{2n_2}{n_1^2 + 4n_2\gamma^q - n_1(n_1^2 + 4n_2\gamma^q)^{1/2}} \ , \tag{17}$$

$$f(\alpha(q)) = \frac{1}{\ln L} \ln\left[\frac{(n_1^2 + 4n_2\gamma^q)^{1/2} - n_1}{2n_2} \right] - \frac{1}{\ln L} \frac{2qn_2\gamma^q \ln\gamma}{n_1^2 + 4n_2\gamma^q - n_1(n_1^2 + 4n_2\gamma^q)^{1/2}} \ . \tag{18}$$

For the Cantor set in Fig. 1 we have

$$D_q = \frac{1}{q-1}\left[q + \frac{1}{\ln 2} \ln\left[\frac{[1 + 4(\frac{3}{4})^q]^{1/2} - 1}{2} \right] \right] \tag{19}$$

and

$$D_{-\infty} = \frac{\ln\frac{1}{3}}{\ln\frac{1}{4}} = 0.7925\ldots , \tag{20}$$

$$D_{\infty} = \frac{\ln\frac{2}{3}}{\ln\frac{1}{2}} = 0.5850\ldots . \tag{21}$$

In Fig. 2 we show D_q and the $f(\alpha)$ spectrum for this Cantor set. The Hausdorff dimension is

$$D_0 = \frac{\ln[(\sqrt{5}+1)/2]}{\ln 2} = 0.6942\ldots . \tag{22}$$

The value $(\sqrt{5}+1)/2$ is the golden mean.

Another soluble example with $l_1 = l_2^2$ is the two-dimensional multifractal in Fig. 3. This set is constructed by the following rule. Start with a square and divide it into 16 pieces. Remove all pieces except the four in the middle, which now form a large square, and the four squares in the corners. Then continue the procedure and divide each of the five squares into five new ones, and so on. For this object $\gamma = \frac{1}{2}$, $d = 2$, $n_1 = 1$, and $n_2 = 4$. D_q is

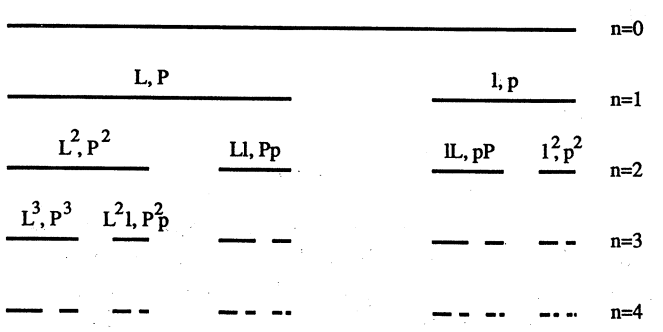

FIG. 1. A Cantor set construction with two rescalings $l_1 = L = \frac{1}{2}$ and $l_2 = l = \frac{1}{4}$ and respective probability rescalings $p_1 = P = \frac{2}{3}$ and $p_2 = p = \frac{1}{3}$. The division of the set continues self-similarly.

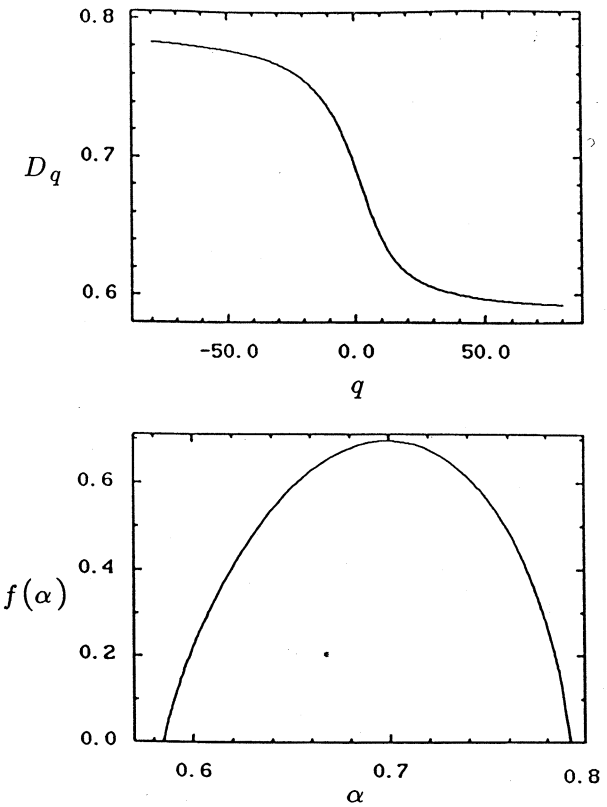

FIG. 2. D_q and the $f(\alpha)$ spectrum for the two-scaled Cantor set in Fig. 1. The zeros of f are $\alpha_{\min} \approx 0.5850$ and $\alpha_{\max} \approx 0.7925$, see text.

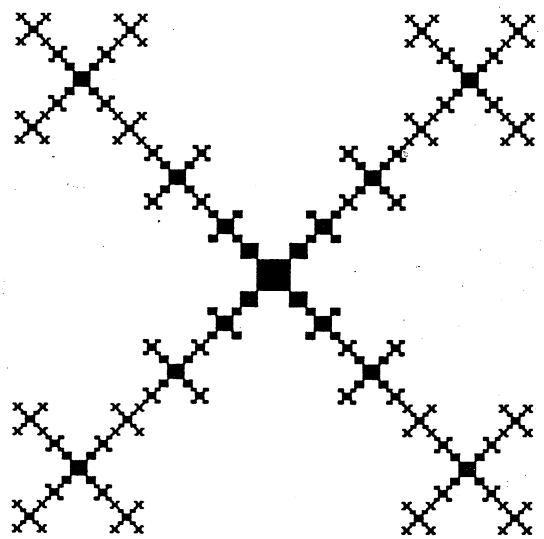

FIG. 3. Example of a two-dimensional fractal with two rescalings. The fractal object is shown on level 4.

then given by

$$D_q=\frac{1}{q-1}\left[2q+\frac{1}{\ln 2}\ln\left[\frac{(1+16\times 2^{-q})^{1/2}-1}{8}\right]\right], \tag{23}$$

and the $f(\alpha)$ spectrum by

$$\alpha(q)=2-\frac{8\times 2^{-q}}{1+16\times 2^{q}-(1+16\times 2^{-q})^{1/2}} \tag{24}$$

$$f(\alpha(q))=\frac{8q\times 2^{-q}}{1+16\times 2^{-q}-(1+16\times 2^{-q})^{1/2}} -\frac{1}{\ln 2}\ln\left[\frac{1+16\times 2^{-q}-(1+16\times 2^{-q})^{1/2}}{8}\right]. \tag{25}$$

The function $\tau(q)$ is shown in Fig. 4, while D_q and the $f(\alpha)$ spectrum are shown in Fig. 5. We can use Eq. (10) in order to understand the shape of $\tau(q)$. Suppose $p_1<p_2$ ($l_1<l_2$) and let $q\to-\infty$. Then the first term will dominate, i.e.,

$$l_1^{\tau}\to n_1 p_1^{q} \tag{26}$$

and

$$\tau(q)\to\frac{\ln n_1+q\ln p_1}{\ln l_1}=qD_{-\infty}-f_{-\infty} \tag{27}$$

by definition. Here $f_{-\infty}=f(\alpha(-\infty))$. For $q\to\infty$ the second term in Eq. (10) dominates and

$$\tau(q)\to\frac{\ln n_2+q\ln p_2}{\ln l_2}=qD_{\infty}-f_{\infty}\ . \tag{28}$$

We now see that the function $\tau(q)$ has two asymptotes with slopes $D_{\infty}=\alpha_{\min}$ and $D_{-\infty}=\alpha_{\max}$, which cross the τ axis at f_{∞} and $f_{-\infty}$, respectively. We also know that $\tau(1)=0$ and $\tau(0)=-D_0=-f_{\max}$. Explicitly, we get for the two limits of α

$$D_{-\infty}=\frac{\ln\frac{1}{8}}{\ln\frac{1}{4}}=\frac{3}{2} \tag{29}$$

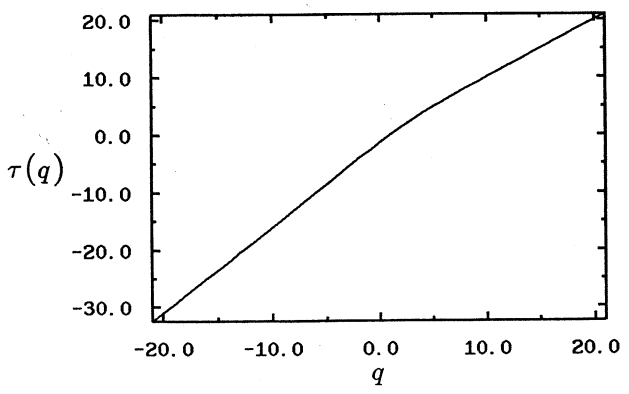

FIG. 4. $\tau(q)$ for the two-dimensional fractal in Fig. 3.

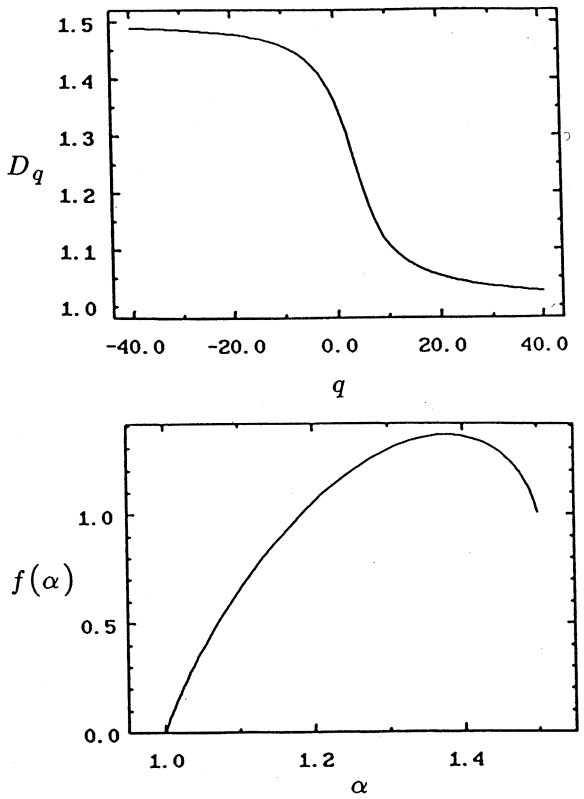

FIG. 5. D_q and $f(\alpha)$ for the two-dimensional fractal in Fig. 3.

and

$$D_{\infty}=\frac{\ln\frac{1}{2}}{\ln\frac{1}{2}}=1\ , \tag{30}$$

and the Hausdorff dimension for this fractal is given by

$$D_0=-\frac{\ln[(\sqrt{17}-1)/8]}{\ln 2}=1.3570\ldots\ . \tag{31}$$

Furthermore, one gets the following limits of f:

$$f_{-\infty}=-\frac{\ln 4}{\ln\frac{1}{4}}=1 \tag{32}$$

and

$$f_{-\infty}=-\frac{\ln 1}{\ln\frac{1}{2}}=0\ . \tag{33}$$

IV. BOX COUNTING

Box counting is maybe the simplest and the most common method to calculate D_q and the $f(\alpha)$ spectrum for a general multifractal. When using box counting we divide the d-dimensional objects into boxes, all with the same size l^d, i.e., $l_i=l$ for all i.

Let N be the total number of nonempty boxes, M the total number of particles (the total mass) and N_i the total number of measures (particles) in the ith box. Then $p_i=N_i/M$. Further suppose that the probabilities are

normalized to give $\Gamma(\tau,q)=1$. We then obtain the following partition sum:

$$\Gamma(\tau,q)=l^{-\tau}\sum_{i=1}^{N}\left[\frac{N_i}{M}\right]^q=1\ . \tag{34}$$

By taking the logarithm of the partition sum we find the relationship between τ and q,

$$\tau(q)=\frac{1}{\ln l}\ln\sum_{i=1}^{N}\left[\frac{N_i}{M}\right]^q, \tag{35}$$

and from Eqs. (6) and (35) we get

$$\alpha(q)=\frac{d\tau}{dq}=\frac{1}{\ln l}\frac{1}{\sum_{i=1}^{N}(N_i/M)^q}\sum_{i=1}^{N}\left[\frac{N_i}{M}\right]^q\ln\frac{N_i}{M}\ . \tag{36}$$

Having τ and α as functions of q, we may now calculate D_q and $f(\alpha)$ from

$$f(\alpha(q))=q\alpha(q)-\tau(q) \tag{37}$$

and

$$D_q=\frac{\tau(q)}{q-1}=\frac{1}{q-1}[q\alpha(q)-f(\alpha(q))]\ . \tag{38}$$

If the N_i are allowed to take fractional values, we see that there will be problems for large negative q; the sum above may be totally dominated by any small N_i and will get a value which strongly depends on the position of the grid.

V. EXACT BOX COUNTING ON A FINITE SET

We will now discuss box counting on different levels of the Cantor set in Fig. 1; the levels $n\in[0,n_r]\subset N$ of the Cantor set will be used to model images with resolutions 4^{-n} for a fractal object whose *finest* resolution (e.g., particle size in an aggregate) is 4^{-n_r}. On a certain level of resolution, the resolution is given by the size of the *smallest* observable (coverable) object and defines the size of the particles out of which the remaining parts of the object are built. Only fully covered particles should be counted; partially covered particles must be excluded in order to avoid terms that blow up for large negative q.

For the simple Cantor set being considered, it is easy to find explicit functions $\tau(q)$, D_q, and an $f(\alpha)$ spectrum on any finite resolution level n of the set and with any box length $l=2^{-(n+m)}$, where $m\in[-n,n]$ labels the size of the boxes on each resolution level. In Fig. 6, a fractal image with a resolution 4^{-3} is modeled by level 3 of the Cantor set. The relevant set of (nonempty) boxes needed to cover this object is also shown in the figure. For a given resolution level n, there are $2n$ different box partitions with box lengths $2^{-(n+m)}$, $m=-n,-n+1,\ldots,n$. On each box level m one gets a spectrum of $n-|m|+1$ different probability measures. Up to box level $m=0$, there are no finite size effects. If $0<m\le n$, some boxes cover parts of the large sized objects consisting of many particles; these boxes thus have a uniform and equal measure. If $m=n$, all boxes contain the same measure and a further subdivision of the boxes will yield no further information.

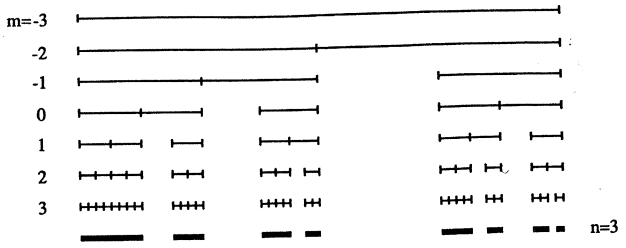

FIG. 6. A fractal with finite resolution given by level 3 of the Cantor set in Fig. 1, together with the relevant box partitions.

The set of boxes can be constructed by a simple procedure. We have two types of boxes, L, covering parts of the image with all of its length, and L', covering a hole with its left half and parts of the image with its right half. On the second level ($m=-n+1$) the set of (nonempty) boxes can thus be represented by (L,L'). When we construct the next level we note that the box L is divided into two new pieces L and L' ($m\le 0$), and L' turns into L; the representation is (L,L',L). When $m>0$ we have to modify the rule since some of the boxes L are divided into two equal parts L.

In order to construct the full box set and calculate the probability measure in the boxes we use the operator $\hat{T}$ and the generators L_k and L_k' having the following properties:

$$\left.\begin{aligned}\hat{T}L_k&=PL_{k-1}+pL_k'\\ \hat{T}L_k'&=L_{k-1}\\ \hat{T}L_0&=2P^{-1}pL_0\end{aligned}\right\}k=1,\ldots,n\ . \tag{39}$$

Here $P=\frac{2}{3}$ and $p=\frac{1}{3}$ build up the probability measures. We may now generate the probability distribution on any box level $m\in[-n,n]$ through

$$\hat{T}^{n+m}L_n \tag{40}$$

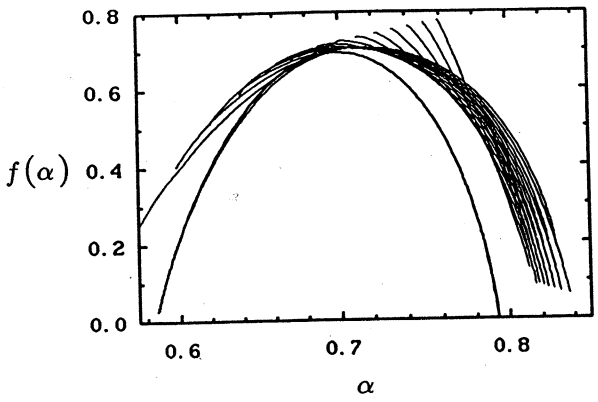

FIG. 7. Exact $f(\alpha)$ spectrum (thick line) compared with the solutions from the box counting with different box sizes on resolution level 16 (thin lines).

by identifying the coefficient and probability measure connected to each L_k and L'_k (L_n represents the initial interval of length one). As an illustration we write the distribution given by $\hat{T}^4 L_3$ for the box level $m=1$ in Fig. 6

$$\hat{T}^4 L_3 = 5P^2 pL_0 + 2Pp^2 L'_1 + p^2 L_1 \ . \tag{41}$$

If we put the probability distribution generated by Eq. (40) into the partition function Eq. (1), we get

$$\Gamma_n^{(m)} = 2^{(n+m)\tau} \sum_{i=|m|+m}^{n+m} n_i^{(m)} (p_i^{(m)})^q \ , \tag{42}$$

where

$$p_i^{(m)} = P^{n+m-i} p^{[(i+1)/2]} \ . \tag{43}$$

The square brackets here denote the integer part. The coefficients $n_i^{(m)}$ are given for $m=-n,\ldots,n$; $i=0,\ldots,n+m$ by the recursion relation

$$n_i^{(m)} = n_{i-1}^{(m-1)} + \epsilon_i (n_i^{(m-1)} + 2\delta_{i-2m} n_{i-2}^{(m-1)}) \ , \tag{44}$$

$$n_0^{(-n)} \equiv 1, \quad n_i^{(m)} \equiv 0, \quad i \notin [0, n+m] \ . \tag{45}$$

The symbols ϵ_i and δ_i in Eq. (44) are defined through

$$\epsilon_i \equiv \begin{cases} 1, & \text{for } i \text{ even} \\ 0, & \text{for } i \text{ odd} \end{cases}$$
$$\delta_i \equiv \begin{cases} 1, & \text{for } i=0 \\ 0, & \text{otherwise} \ . \end{cases} \tag{46}$$

With the partition function known on any box level on any level of resolution of the Cantor set, we can now construct the scaling functions

$$\tau_n^{(m)}(q) = -\frac{1}{(n+m)\ln 2} \ln \Sigma_a^{(m)} \ , \tag{47}$$

$$(D_n^{(m)})_q = \frac{\tau_n^{(m)}(q)}{q-1} \ , \tag{48}$$

$$\alpha_n^{(m)}(q) = -\frac{1}{(n+m)\ln 2} \frac{\Sigma_A^{(m)}}{\Sigma_a^{(m)}} \ , \tag{49}$$

$$f_n^{(m)}(\alpha_n^{(m)}(q)) = q\alpha_n^{(m)}(q) - \tau_n^{(m)}(q) \ , \tag{50}$$

where

$$\Sigma_a^{(m)} = \sum_{i=|m|+m}^{n+m} n_i^{(m)} (p_i^{(m)})^q \ ,$$
$$\Sigma_A^{(m)} = \sum_{i=|m|+m}^{n+m} n_i^{(m)} (p_i^{(m)})^q \ln(p_i^{(m)}) \ . \tag{51}$$

In Fig. 7 we show the exact $f(\alpha)$ curve and successive approximations $f_n^{(m)}(\alpha_n^{(m)})$, for $n=16$ and $m=0,1,2,\ldots,15$ [$f_{16}^{(16)}$ just gives a single point at $(D_{-\infty}, D_{-\infty})$]. Note that the curves from the box-counting calculation cross each other. We observe that for large negative q, $f_{16}^{(15)}$ is the best approximation. When decreasing the magnitude of $|q|$, the $f_{16}^{(14)}$ curve crosses $f_{16}^{(15)}$ and becomes the best approximation. If we continue to decrease $|q|$, $f_{16}^{(13)}$ crosses the $f_{16}^{(14)}$ curve and so on until $f_{16}^{(0)}$ crosses $f_{16}^{(1)}$. The optimal box size therefore depends on the value of q. For positive q values, $f_{16}^{(0)}$ is the most accurate approximation for all q, and the curves $f_{16}^{(m)}$, $m<0$ will all be on the right-hand side of $f_{16}^{(0)}$.

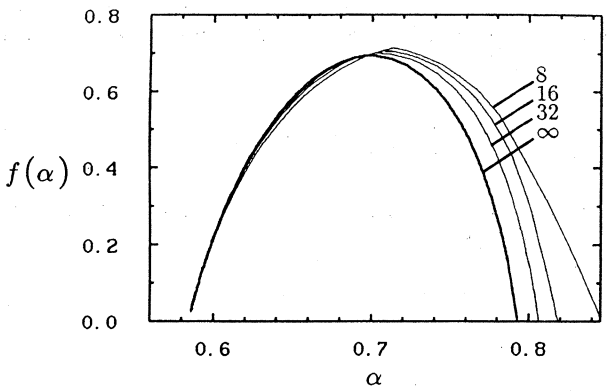

FIG. 8. Exact $f(\alpha)$ spectrum compared with successive, optimal approximations on different levels of resolution. The thin curves are f_8^*, f_{16}^*, and f_{32}^*.

The main conclusion of the above results is that if we want to approximate $f(\alpha)$ for the Cantor set with box counting at a finite level n, we should (i) let the envelope of the curves $f_n^{(m)}(\alpha)$, $m=0,1,\ldots,n-1$ approximate $f(\alpha)$ for negative q, i.e., we select the left-most curve for negative q values by calculating the crossing points of the curves, and (ii) let $f_n^{(0)}(\alpha)$ approximate $f(\alpha)$ for all positive q. The optimal $f(\alpha)$ spectrum thus obtained, $f_n^*(\alpha)$, is shown in Fig. 8 for $n=8$, 16, and 32 compared with the exact curve. We have that $\lim_{n\to\infty} f_n^* = f$.

To illustrate the convergence of the Hausdorff dimension we have in Fig. 9 plotted D_0 as a function of the box size on level 32. Note the fast convergence for small boxes. The minimum of the curve is the best approximation of the Hausdorff dimension. Also note that the exact value of $D_{-\infty}$ can be found by calculating D_0 with a box size l of the same size as the smallest interval in the set.

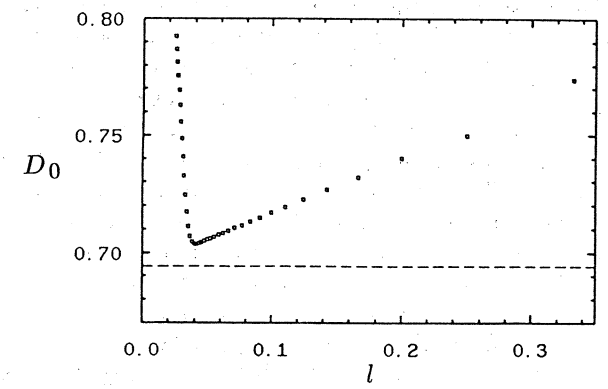

FIG. 9. Successive approximations of the Hausdorff dimension D_0 plotted vs the box size l on level 32. The dashed line represents the exact value.

VI. CONCLUSIONS

We have used a Cantor set at finite levels to model a finite fractal. The simple choice of length scales of the Cantor set made it possible to find the generalized dimensions and the spectrum of scaling indices analytically. For this particular choice we have also been able to solve the complete box-counting problem. By comparing the box-counting solution with the exact one we find a relationship between the value of q and the size of the boxes giving the most accurate result. For positive q, the best result is obtained for a grid size equal to the size of the largest connected object, i.e., the length scale where finite-size effects begin to play a role. For negative q, the influence of finite sizes is crucial for the determination of the $f(\alpha)$ spectrum, such that all the way down to the particle level of resolution, each partition level (box size) gives a contribution in a corresponding q interval.

[1]A. Renyi, *Probability Theory* (North-Holland, Amsterdam, 1970).
[2]P. Grassberger, Phys. Lett. **97A**, 227 (1983).
[3]H. G. E. Hentschel and I. Procaccia, Physica D **8**, 435 (1983).
[4]T. C. Halsey, M. H. Jensen, L. P. Kadanoff, I. Procaccia, and B. I. Shraiman, Phys. Rev. A **33**, 1141 (1986).
[5]G. A. Niklasson, A. Torebring, C. Larsson, C. G. Granqvist, and T. Farestam, Phys. Rev. Lett. **60**, 1735 (1988).
[6]C. Amitranto, A. Conigoli, and F. di Liberto, Phys. Rev. Lett. **57**, 1098 (1986).
[7]K. J. Måløy, F. Boger, J. Feder, and T. Jøssang, in *Time-Dependent Effects in Disordered Materials,* edited by R. Pynn and T. Riste (Plenum, New York, 1987), p. 111.
[8]J. Nittmann, H. E. Stanley, E. Toubol, and G. Daccord, Phys. Rev. Lett. **58**, 619 (1987).
[9]A. Choen and I. Procaccia, Phys. Rev. A **31**, 1872 (1985).